Open-Circuit Voltage Measurement of Lithium-Iron-Phosphate Batteries

F. Baronti*, W. Zamboni§ , R. Roncella*, R. Saletti*, and G. Spagnuolo§
*Dipartimento di Ingegneria dell'Informazione, Università di Pisa, I-56122 Pisa, Italy
e-mail: f.baronti@iet.unipi.it
§Dipartimento di Ingegneria dell'Informazione, Ingegneria Elettrica e Matematica Applicata (DIEM)
Università degli Studi di Salerno, I-84084 Fisciano (SA), Italy
e-mail wzamboni@unisa.it

***Abstract*—This paper evaluates some techniques for the reduction of the measuring time required to obtain an accurate and exhaustive characterisation of the Open-Circuit Voltage (OCV) of a Lithium-Iron-Phosphate ($LiFePO_4$) battery. The OCV is a very important parameter of a battery equivalent electrical model, typically used in the model-based design of a battery management system. OCV characterisation is quite a time consuming task, as OCV relaxation lasts for several minutes or hours after the battery current is interrupted. This task is especially challenging in a $LiFePO_4$ battery, as the latter shows pronounced hysteresis, which dramatically increases the number of OCV points to be measured. In order to reduce the measuring time, we investigate the OCV independence from the current rate at which the state-of-charge is adjusted and the possibility to predict the fully relaxed OCV value by modelling the relaxation phenomenon.**

I. Introduction

The capability of reproducing the battery's behaviour in an accurate way plays a central role in the model-based design of a battery system [1] and the relevant Battery Management System (BMS) [2], [3]. A common way to mimic the battery terminal voltage is by means of an equivalent electrical circuit derived from the classical Randles' model [4]. This model includes the series of a voltage generator to reproduce the Open-Circuit Voltage (OCV), a resistor and one or more R-C branches with different time constants to account for the internal impedance of the battery and the relaxation phenomena occurring when the battery current is interrupted. Usually, two R-C branches with time constants in the range of seconds and minutes are sufficient to reproduce the battery dynamic behaviour in a way accurate enough for control purposes in a BMS [4], [5]. The values of the R-C parameters can be identified offline by means of electrochemical impedance spectroscopy [6] or pulsed current tests [4], [5] or during the battery operation using, for instance, the Extended Kalman filter or the Moving Window Least Squares method [7], [8].

An accurate and exhaustive characterisation of the OCV generator is far from being a simple task as relaxation phenomena last several minutes or even hours after the current is interrupted. This is even more complicated in lithium-ion batteries using $LiFePO_4$-based active materials for the cathode electrode. In the State-of-Charge (SoC) versus OCV plane, these batteries exhibit an OCV discharge curve lying well below the charge curve. This phenomenon is called hysteresis [9], [10].

OCV measurements are usually performed by bringing the battery to a known state, typically the full-charge, *i.e.* at $100\,\%$ of SoC, and then by gradually altering the SoC with a constant current pulse followed by a rest time. The OCV is measured at the end of the rest time (or extrapolated by fitting the OCV behaviour during the rest). If SoC is gradually brought to 0 and then to $100\,\%$ again (full-discharge/full-charge test, FDFC), we obtain a complete OCV characterisation of a battery, or a major loop if the battery shows hysteresis. The incremental charge/discharge method is considered more reliable in accounting for the open-circuit potential of the battery's electrodes, compared to a continuous charge/discharge cycle at very low currents (much less than 1C rate, where 1C rate means a current that will discharge a fully charged battery in 1 h) [11]. In fact, an incremental charge/discharge approach with $5\,\%$ SoC variation and a rest time between 1 h and 3 h provides a very good approximation of the $\mathrm{SoC} - \mathrm{OCV}$ relationship [9], [11].

An exhaustive OCV characterisation of batteries showing hysteresis requires the measurement of several branches within the major loop in order to accurately reconstruct any OCV evolution corresponding to the full history of the SoC [12]. This results in a very time consuming procedure. Thus, any factor allowing a valuable reduction of this long characterisation time is worth being investigated.

We note that the measuring time of each OCV point is the sum of the time t_{on} required to establish the SoC variation and the rest time t_{rest}. The first contribution is inversely proportional to the current value. For instance, to achieve a $5\,\%$ SoC variation, this time decreases from 30 min to 3 min when the current value is increased from 0.1C rate to 1C rate. Thus, in order to save time by reducing t_{on}, it is interesting to determine whether or not the current rate used to adjust the SoC changes the OCV curve. If a rate independence is observed, its upper limit of validity should be found. The rate-dependence of the hysteresis loop has only been very partially faced in the literature. In particular, the behaviour of the OCV when $\mathrm{SoC} = 50\,\%$ is adjusted from full charge and full discharge at 0.5C rate and 10C rate is analysed in [13], showing that the hysteresis is significantly reduced at the

978-1-4799-6144-6/15/$31.00 ©2015 IEEE

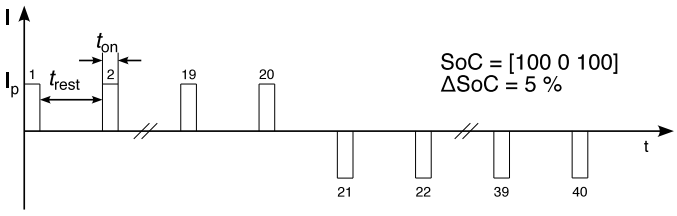

Fig. 1. Example of a Pulse Current Test for the measurement of the major loop with a State-of-Charge resolution of 5 %.

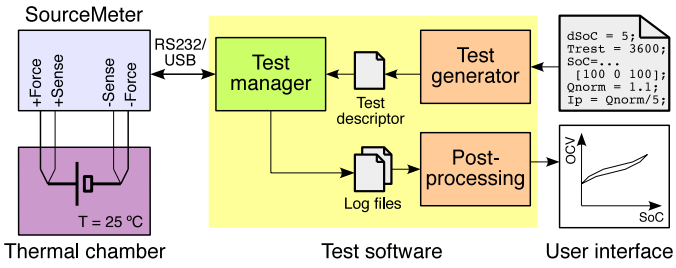

Fig. 2. Schematic diagram of the experimental set-up.

higher C-rate, but nothing has been done for typical operating currents around 1C rate.

Another way to shorten the characterisation time is to reduce the rest time $t_{\rm rest}$. A very simple relaxation model for OCV is proposed in [9], allowing, in principle, to reduce $t_{\rm rest}$ to some minutes and predict its relaxation to some hours.

This work aims at providing an in depth analysis of the $\mathrm{SoC}-\mathrm{OCV}$ hysteretic characteristics of a $LiFePO_4$ cell, facing the issues related to the rate-independence (limited to the the interval from 0.1C up to 3C) and the effective predictability of the hysteresis relaxation. Before proceeding with the analysis, some details of the automated test procedure and the rules for processing the time-domain data to obtain $\mathrm{SoC}-\mathrm{OCV}$ curves are discussed.

II. Methodology

As stated above, the measurements typically used to extract the relationship between OCV and SoC requires a well-defined, automatised, and accurate test procedure, as they are very time consuming and sensitive to external disturbances. Thus, the availability of a specialised and reliable experimental set-up is of crucial importance.

A. Experimental set-up

The experimental set-up is designed to carry out Pulsed Current Tests (PCTs). A PCT is a sequence of current pulses, each of them determining a given SoC variation at a constant rate, separated by a rest time. A PCT for the measurement of the hysteresis major loop is shown in Fig. 1. The version of the experimental set-up used in this work is an enhancement of that described in [10], as the test procedure is fully automised. Indeed, the user needs to provide just a few parameters to configure a PCT, whereas all the required operations are automatically carried out by the developed test software. The *test parameters* to be provided are:

- the cell normalisation charge $Q_{\rm norm}$ (usually the nominal capacity of the cell under test);
- the cell cut-off charge/discharge voltages $V_{\rm thres,c}$ and $V_{\rm thres,d}$;
- the desired SoC history;
- the SoC history resolution, *i.e.*, ΔSoC;
- the SoC variation speed, *i.e.*, the amplitude of the current pulse I_p;
- the value of the rest time $t_{\rm rest}$.

Note that $t_{\rm on} = Q_{\rm norm}\Delta\mathrm{SoC}\, I_p^{-1}$.

The *test parameters* are the inputs of the *test software*, which is responsible for the execution of a PCT, as shown in Fig. 2. A PCT is implemented as a sequence of elementary test steps, which consist of *charge*, *discharge* and *rest* operations with configurable parameters. The *charge/discharge* step produces a positive/negative variation ΔSoC of the cell SoC at a constant current (the current is assumed positive for discharge). The configuration parameters include the charge/discharge current, the step duration, and the target charge/discharge voltage. A step can end because the cell voltage reaches the target value or the current drops below a given percentage of the set value, thus implementing the constant current (CC) and the constant voltage (CV) phases for a full-discharge/full-charge (FDFC) of the cell. The CV phase occurs whenever the target SoC value is either 0 % or 100 %.

The step sequence and the relevant configuration parameters are automatically generated by the *test generator* script, starting from the PCT parameters, and saved in the *test descriptor* file, as shown in Fig. 2. This avoids errors in the manual writing of the file, so that the *test generator* piece of software provides a valuable improvement of OCV characterisation with respect to the set-up used in [10] and the "automated measurement station for battery testing" proposed in [14].

The test descriptor file is the input of the *test manager* LabVIEW application. The latter controls the execution of the test steps, which are performed by means of a Keithley 2420 SourceMeter Unit (SMU). This instrument generates the cell current (either as current source or sink) and measures the cell current and voltage with a four-wire connection to the cell. The voltage measurement is obtained with an accuracy better than 1.5 mV in the full cell voltage range. The cell is placed inside a thermal chamber Binder MK53, by which the cell's ambient temperature T is kept constant at $T = 298$ K. This is an important feature, not available in [14], as the battery behaviour strongly depends on the operating temperature [5].

It is worth noting that an *Initialisation phase* is used to ensure the "same" starting point for every PCT. This phase includes a full battery discharge, a 1 h rest and a full recharge followed by another 4 h rest.

The Test Manager application communicates with the SMU via a RS232/USB link in order to configure the instrument and to acquire the measured values of the cell current and voltage. These values are saved in the *log file* relevant to the current step. The sampling rate is set to 0.5 Hz. This value

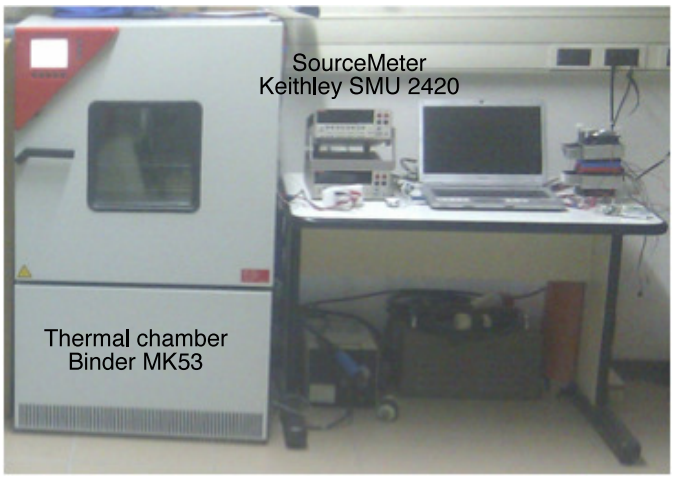

Fig. 3. Photograph of the experimental set-up.

is suitable for capturing OCV relaxation phenomena, avoiding the useless generation of large log files, as a PCT may last for some days. The set of log files belonging to a PCT are then sent to a *post-processing* function to obtain the required $\mathrm{OCV}-\mathrm{SoC}$ relationship. Details of the postprocessing will be given in the following section. The test generator and the post-processing software functions are implemented as MATLAB® scripts. Fig. 3 shows a picture of the experimental set-up.

The cell under test is a brand-new $1.1\,\mathrm{A\,h}$ $LiFePO_4$ cell (A123's APR18650-M1 cell). The charge/discharge cut-off voltages are $V_{\mathrm{thres,c}} = 3.6\,\mathrm{V}$ and $V_{\mathrm{thres,d}} = 2.0\,\mathrm{V}$, respectively. The recommended standard charge current for the tested cell is $1.5\,\mathrm{A}$ and the maximum continuous discharge current is $30\,\mathrm{A}$. The cell was first conditioned by ten full charge/discharge cycles, after the delivery from the manufacturer.

B. Post-processing

The function of post-processing is the extraction of the $\mathrm{SoC}-\mathrm{OCV}$ relationship from the log files of a PCT, according to the operative definitions of these two "abstract" quantities given afterwords.

1) OCV definition: OCV is usually defined as the cell's terminal voltage at the end of the rest step. However, the user can also choose to extract another value before the end of the rest period.

2) SoC definition: The SoC of a cell is a normalised representation of the residual "charge" (in the sense of energy) that can be extracted from the battery until it is completely discharged. From a theoretical point of view, this definition requires to completely discharge the battery with a lossless thermodynamical process (infinitesimal currents) and to measure the extracted energy (for instance, see [15]). The battery is considered fully-charged (-discharged) when the fixed threshold $V_{\mathrm{thres,c}}$ (or $V_{\mathrm{thres,d}}$) is reached *at zero current* in the CV phase. According to this definition, it is theoretically impossible to measure the SoC without perturbing the battery state.

From a practical point of view, provided an accurate measurement of the battery current i, the SoC variation $\Delta\mathrm{SoC}$ can be monitored by computing the electric charge exchanged at the cell's terminals. Full-charge (-discharge) states are defined by accepting that the CV current goes below *an arbitrary fixed threshold* (typically C/30 rate). Then, the charge exchanged is normalised and a "reasonable" SoC from v and i time-measurements is obtained.

Following this approach, first we compute the electric charge ΔQ exchanged by the battery as a function of time by integrating (in discrete time) the current $i(t)$ using the trapezoidal integration rule:

$$\Delta Q(t_k) = \sum_{j=1}^{k} \frac{i(t_j) + i(t_{j-1})}{2} \left(t_j - t_{j-1}\right), \qquad (1)$$

being t_k a generic discrete time instant and t_0 the initial time. Then, chosen a normalisation constant Q_{norm} and knowing the initial state SoC_0 (for instance, starting from the full-charge condition), the SoC can be expressed as a function of time:

$$\mathrm{SoC}(t_k) = \mathrm{SoC}_0 - \frac{\Delta Q(t_k)}{Q_{\mathrm{norm}}}. \qquad (2)$$

The value used for Q_{norm} is usually the cell nominal capacity Q_n and this choice is also adopted in this paper. This may lead to SoC values outside the expected interval $[0, 1]$ [10], if the charge span in a FDFC cycle is greater than the nominal value. In this work, we have found that Q_n is slightly higher than the maximum charge that can be injected or extracted from the battery in all the performed tests.

The above described SoC definition, simply called Coulomb Counting, holds for all $t > 0$ and does not take into account any information coming from the voltage measurements. Moreover, it is worth noticing that errors might accumulate during the integration process. A very basic correction can be adopted while processing PCT data. During a PCT, some full-charge/discharge state might be detected (the test goes in CV mode), and it is possible to use these points as "reset points" for the integration (1). From a practical point of view, (2) keeps holding in any interval between full-charge and full-discharge state (or vice versa) and undergoes a reset when the full-charge/discharge is detected.

The described approaches lead to small differences in the SoC–OCV characteristic to be reconstructed. The two methods are compared in Fig. 4. PCT data for a FDFC loop test at 0.5C current rate are processed both with the Coulomb Counting approach and with Coulomb Counting/Reset Points method.

III. Rate-independence of the OCV hysteresis

The first set of tests investigate the dependence of the hysteresis major loop on the current rate. To have a more detailed insight into such a dependence, the cell has been stimulated with four FDFC loop tests, drawing a clockwise major loop in the SoC–OCV plane. The tests were designed to inject/extract a 5 % charge at each pulse (with the exception of the pulses approaching the full-charge/discharge condition,

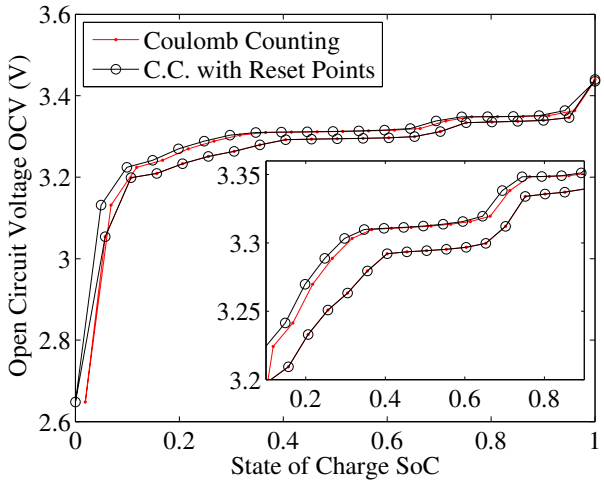

Fig. 4. Full discharge-charge loop for current rate C/2: comparison between the Coulomb Counting approach (·) and the Coulomb Counting with Reset Points method (○). The inset highlights that small deviations occur between the charge curves.

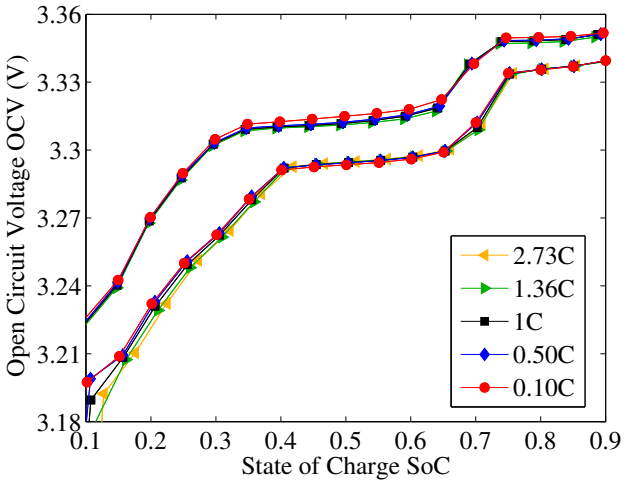

Fig. 5. Hysteresis major loop for various current rates: 0.1C (equal to 110 mA), 0.5 C (equal to 550 mA), 1C (equal to 1.10 A), 1.36 C (equal to 1.50 A), and 2.73C (equal to 3.00 A). The 3 A curve has been reported for the discharge phase only.

TABLE I
HYSTERESIS RATE-INDEPENDENCE TESTS.

current C-rate	pulse current	t_{on}	t_{rest}
2.72C	3.00 A	66 s	1 h (*)
1.37C	1.50 A	132 s	1 h
1C	1.10 A	3 min	1 h
0.5C	550 mA	6 min	1 h
0.1C	110 mA	30 min	1 h

(*) discharge only

where the charge exchanged cannot be determined *a priori* because of the CV phase). The rest time is kept fixed at 1 h, while the pulse duration t_{on} is automatically set by the test generator in correspondence of the current rate. Test details are given in TABLE I.

The results of the test are reported in Fig. 5. The rate-independence of the hysteresis major loop is confirmed with good accuracy in all the performed tests, *i.e.* up to 2.72C rate in discharge and up to 1.37C rate in charge.

IV. HYSTERESIS RELAXATION

It is well known that battery OCV relaxes over time with a monotonic behaviour. Here, we investigate with PCT tests what happens to the time evolution of the hysteresis loop at a fixed current rate and different rest times.

Experimental results achieved by 5 % PCTs performed at 1C current rate are reported in Fig. 6. We have found that the hysteresis major loop relaxes (*i.e.*, becomes narrower) with time and is bounded by a limit loop. The experimental behaviour agrees with what has been reported in [9], where the hysteresis loop after 3 h rest time is assumed as the relaxed state.

In Fig. 6 we notice that the OCV relaxation is almost completed after a rest time equal to 1 h, far less than what is stated in [9] (3 h). The maximum variation associated to

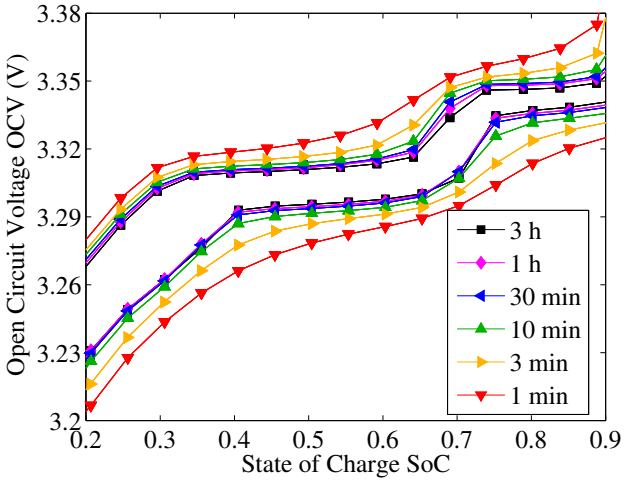

Fig. 6. Hysteresis major loop at 1C current rate for various rest times.

relaxation phenomena between t_{rest} =1 h and 3 h is below 3 mV, which less than 10 % of what is observed by comparing t_{rest} =1 min and 3 h (approximately 32 mV).

It is interesting to investigate whether the OCV relaxation can be predicted by a closed-form equation over the whole range of SoC. As mentioned in the Introduction, a very simple and attractive relaxation model has been proposed in [9], which is worth being applied to the experimental data reported here. According to that model, for each fixed SoC value, the OCV relaxes towards its stationary value OCV_∞ according to the following equation:

$$\mathrm{OCV}(t) = \mathrm{OCV}_\infty + (\mathrm{OCV}_0 - \mathrm{OCV}_\infty)\, e^{-\frac{t}{\tau}}, \qquad (3)$$

where OCV_0 is a known parameter representing the relaxation starting point. Experimental OCV taken at t_{rest} = 3 h and

$t_{\rm rest} = 1$ min can be used as OCV_∞ and OCV_0, respectively, whereas τ is a fitting parameter.

In order to determine the value of the fitting parameter τ (both for discharge and charge mode), the experimental OCV curves at various $t_{\rm rest}$ have been interpolated using splines and then resampled on a regularly-spaced grid along the SoC axis (every $\Delta\mathrm{SoC} = 1$ %), to allow the fitting for a fixed SoC value. The fitting is performed both for discharge and charge OCV, using (3) to compute τ with a least-square identification algorithm. The extraction of τ is very sensitive to the SoC considered, as depicted in Fig. 7.

The fitting function (using the mean values of τ determined as in Fig. 7) is plotted together with the experimental data in Fig. 8, to evaluate the accuracy of the reconstruction of the OCV relaxation in the time interval $[1\,\mathrm{min}, 3\,\mathrm{h}]$. The figure shows that the exponential fitting is rather close to the experimental data, but some errors are clearly visible. This means that the OCV relation phenomenon cannot be accurately modelled with a single exponential, as proposed in [9].

As a matter of fact, it is difficult to set up a fitting expression modelling the relaxation of the OCV curves and, thus, the hysteresis major loop. Alternative fitting formulas using hyperbolic functions or more than one exponential terms have also been also tested, yielding similar unsatisfactory results.

V. Conclusion and Future Work

In this paper we have firstly proven the rate-independence of the SoC–OCV hysteresis major loop in lithium-iron-phosphate batteries. This is a valuable result that can be used to speed-up the OCV characterisation of a $\mathrm{LiFePO_4}$ battery. The second important result of this work is that the use of a closed-form equation and a fitting procedure do not yield a very accurate prediction of the OCV relaxation over time. Thus, it seems unfeasible to attain an accurate OCV characterisation by directly extrapolating the fully relaxed OCV values from a pulsed current test with a short rest time (on the order of a few minutes) between pulses. This is an important result, as other authors have suggested that this method could be used to reduce the OCV measurement time [11].

However, if we recall Fig. 6, we can note that the OCV values measured with $t_{\rm rest} = 10\,\mathrm{min}$ are relatively close to the corresponding fully relaxed values. In fact, their maximum and rms deviation are $8.1\,\mathrm{mV}$ and $3.7\,\mathrm{mV}$, respectively, when SoC varies from $15\,\%$ to $85\,\%$ (which is the typical SoC span in many applications). These deviation values are close to the precision obtained in OCV measurements, in which a variability on the order of a few millivolt is observed from one experiment to another. Thus, PCTs with a $10\,\mathrm{min}$ rest time can provide a good approximation of the SoC–OCV relationship. This fact is particularly attractive for long characterisation of the battery involving several minor loops, such as the so-called first-order reversal (FOR) branches, used to identify hysteresis operators [12].

As a preliminary validation of this conclusion, we carried out a PCT in which SoC was varied from $100\,\%$ down to $40\,\%$, then up to $60\,\%$ and finally down to $0\,\%$ (thus drawing a minor loop), with both $t_{\rm rest} = 10\,\mathrm{min}$ and $t_{\rm rest} = 1\,\mathrm{h}$. The maximum and rms deviation of the OCV values obtained with the short and long rest times are $5.6\,\mathrm{mV}$ and $2.6\,\mathrm{mV}$, respectively, considering again the SoC range from $15\,\%$ to $85\,\%$. This confirms that $t_{\rm rest} = 10\,\mathrm{min}$ can provide a good approximation of the fully relaxed OCV value, while significantly shortening the measurement time.

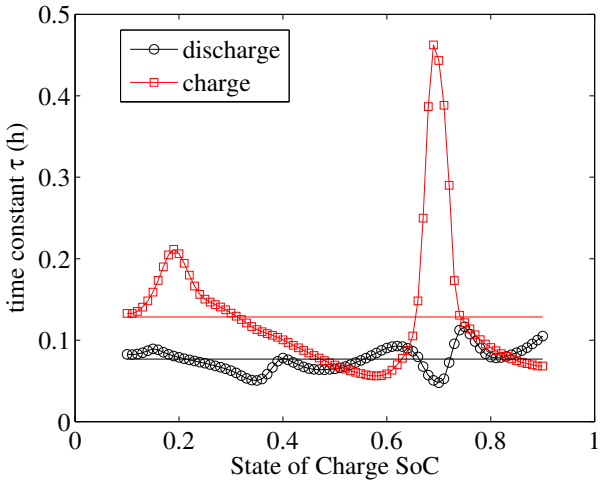

Fig. 7. Fitting parameter τ (discharge and charge phase) as a function of SoC. Horizontal lines represent the mean values $\tau_{\mathrm{d,av}}$ and $\tau_{\mathrm{c,av}}$ computed for $\mathrm{SoC} \in [10\,\%, 90\,\%]$. These mean values are used as fitting parameters of the OCV relaxation.

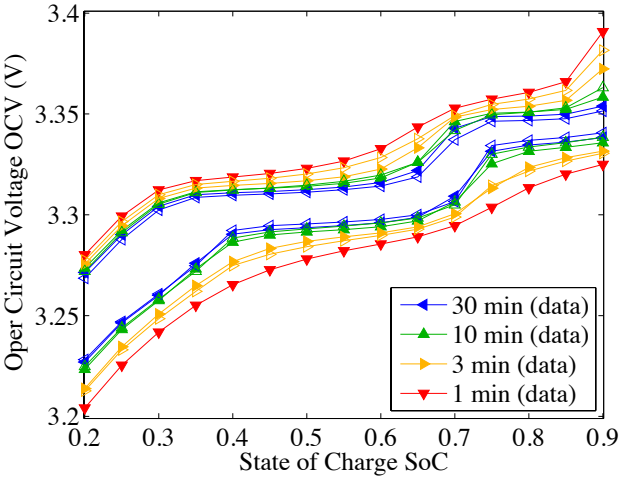

Fig. 8. Reconstruction of the OCV relaxation by using the model (3) for four values of the relaxation time. The fitted data (empty markers) are plotted together with the experimental data (full markers).

References

[1] X. Hu, R. Xiong, and B. Egardt, "Model-Based Dynamic Power Assessment of Lithium-Ion Batteries Considering Different Operating Conditions," *IEEE Transactions on Industrial Informatics*, vol. 10, no. 3, pp. 1948–1959, Aug. 2014.

[2] L. Lu, X. Han, J. Li, J. Hua, and M. Ouyang, "A review on the key issues for lithium-ion battery management in electric vehicles," *Journal of Power Sources*, vol. 226, pp. 272–288, Mar. 2013.

[3] H. Rahimi-Eichi, U. Ojha, F. Baronti, and M.-Y. Chow, "Battery Management System: An Overview of Its Application in the Smart Grid and Electric Vehicles," *IEEE Industrial Electronics Magazine*, vol. 7, no. 2, pp. 4–16, Jun. 2013.

[4] M. Chen and G. Rincon-Mora, "Accurate Electrical Battery Model Capable of Predicting Runtime and I-V Performance," *IEEE Transactions on Energy Conversion*, vol. 21, no. 2, pp. 504–511, Jun. 2006.

[5] F. Baronti, G. Fantechi, E. Leonardi, R. Roncella, and R. Saletti, "Enhanced model for Lithium-Polymer cells including temperature effects," in *IECON 2010 - 36th Annual Conference on IEEE Industrial Electronics Society*. IEEE, Nov. 2010, pp. 2329–2333.

[6] P. Buschel, T. Gunther, and O. Kanoun, "Distribution of relaxation times for effect identification and modeling of impedance spectra," in *2014 IEEE International Instrumentation and Measurement Technology Conference (I2MTC)*. IEEE, May 2014, pp. 901–904.

[7] F. Baronti, W. Zamboni, N. Femia, H. Rahimi-Eichi, R. Roncella, S. Rosi, R. Saletti, and M.-Y. Chow, "Parameter identification of Li-Po batteries in electric vehicles: A comparative study," in *2013 IEEE International Symposium on Industrial Electronics*. IEEE, May 2013, pp. 1–7.

[8] R. Restaino and W. Zamboni, "Rao-blackwellised particle filter for battery state-of-charge and parameters estimation," in *IECON 2013 - 39th Annual Conference of the IEEE Industrial Electronics Society*. IEEE, Nov. 2013, pp. 6783–6788.

[9] M. A. Roscher and D. U. Sauer, "Dynamic electric behavior and open-circuit-voltage modeling of LiFePO4-based lithium ion secondary batteries," *Journal of Power Sources*, vol. 196, no. 1, pp. 331–336, 2011.

[10] F. Baronti, W. Zamboni, N. Femia, R. Roncella, and R. Saletti, "Experimental analysis of open-circuit voltage hysteresis in lithium-iron-phosphate batteries," in *IECON 2013 - 39th Annual Conference of the IEEE Industrial Electronics Society*. IEEE, Nov. 2013, pp. 6728–6733.

[11] M. Petzl and M. A. Danzer, "Advancements in OCV Measurement and Analysis for Lithium-Ion Batteries," *IEEE Transactions on Energy Conversion*, vol. 28, no. 3, pp. 675–681, Sep. 2013.

[12] F. Baronti, N. Femia, R. Saleti, C. Visone, and W. Zamboni, "Hysteresis Modelling in Li-ion Batteries," *IEEE Transactions on Magnetics*, vol. 50, no. 11, pp. 1–4, Nov. 2014.

[13] M. A. Roscher, O. Bohlen, and J. Vetter, "OCV Hysteresis in Li-Ion Batteries including Two-Phase Transition Materials," *International Journal of Electrochemistry*, vol. 2011, pp. 1–6, 2011.

[14] D. Gallo, C. Landi, M. Luiso, A. Rosano, M. Landi, and V. Paciello, "Testing protocols for battery characterization," in *2014 IEEE International Instrumentation and Measurement Technology Conference (I2MTC) Proceedings*. IEEE, May 2014, pp. 374–379.

[15] G. L. Plett, "Extended Kalman filtering for battery management systems of LiPB-based HEV battery packs: Part 2. Modeling and identification," *Journal of Power Sources*, vol. 134, no. 2, pp. 262–276, 2004.